Prepared in JHEP format

Validation of next-to-leading order QCD for lepton collisions

Felix Tellander

Department of Astronomy and Theoretical Physics,
Lund University, SE-223 62 Lund, Sweden

E-mail: felix@tellander.se

Abstract: In this paper we present a validation of a sample of cross sections for the current developement version of the Monte Carlo event generator WHIZARD. The cross sections are calculated for a future linear lepton collider including contributions up to next-to-leading order (NLO) in perturbative QCD. With a couple of discrepancies, the obtained results agree well with other calculations. Moreover we discuss the cancelation of divergences at NLO and show how it works for $t\bar{t}$-production.

Keywords: NLO computation, lepton collisions, top quark physics

Contents

1 Introduction

In high energy collision experiments there is a constant compromise between energy and precisions. Hadron colliders, such as the Large Hadron Collider (LHC) in CERN, allows for extremely high energy collisions with $\sqrt{s} = 13$ TeV. However, the drawback is that the colliding protons are dynamical systems consisting of a sea of quarks and gluons for which the properties are not known from first principles. Lepton colliders on the other hand, provide a much cleaner environment since the electrons (the particle that realistically would be used in a lepton collider) in the Standard Model (SM) are fundamental particles. The draw back for lepton colliders are that in circular machines they emit so much synchrotron radiation that they would evaporate at high energies. Future lepton colliders must therefore be linear machines such as the proposed International Linear Collider (ILC) [1] or Compact Linear Collider (CLIC) [2]. A future lepton collider would provide unprecedented precision for measurements in the electroweak, top and Higgs sectors.

The top quark is the heaviest particle in the SM and is therefore of special interest. Because of its large mass, the top quark together with the Higgs boson are crucial for the stability problem of the electroweak vacuum [3, 4] and exact determination of its mass and Yukawa coupling to Higgs boson is therefore desirable. Due to its large mass, the top quark decays before hadronization via $t \to bW$, where the W boson continues to decay while the b-quark hadronizes and can be identified as a tagged jet. The lack of hadronic background

in lepton collisions makes the reconstruction of the b-jet reasonably easy and precise in this situation [5].

In this paper we do not only study $t\bar{t}$ and $t\bar{t}H$ production in lepton collisions but we do a general validation of different processes at next-to-leading order (NLO) QCD for the multi-purpose event generator WHIZARD [6, 7] which is extended to preform automated NLO calculations. The one-loop contributions are calculated with OpenLoops [8] and compared to MadGraph5_aMC@NLO [9]. This is done using the current development version of WHIZARD to make sure no errors have appeared in the new versions of the code.

This paper is organized as follows. In the following section we introduce WHIZARD and NLO calculations using OpenLoops. In section 3 we discuss top quark physics and especially how to deal with singularities at NLO. Following this we show the input parameters and the results in section 4 and make some concluding remarks in section 5.

2 Calculation setup

2.1 WHIZARD at NLO

The multi-purpose event generator WHIZARD is designed to work both for hadron and lepton collisions, on its own it can deal with arbitrary SM processes and many beyond the Standard Model (BSM) processes at tree level. Furthermore, it can treat many processes at NLO. WHIZARD consists of many components, some of the most important are O'MEGA [6], VAMP [10] and CIRCE [11]. The matrix elements are calculated by O'MEGA, they are calculated as helicity amplitudes to avoid the use of Feynman diagrams. VAMP preforms Monte Carlo integration and grid sampling while CIRCE defines and evaluates lepton beam spectra.

The treatment of NLO calculations are based on the FKS subtraction scheme [12, 13]. A simple description of this is the following; it partitions the phase space into regions where only one divergent configuration in each and these are then regulated by plus-distributions. In this work OpenLoops has been used as one-loop matrix provider.

2.2 OpenLoops

OpenLoops [8] provides all necessary Born and one-loop amplitudes together with colour and helicity correlators required by the FKS subtraction scheme. The regularization of hard (UV) and soft (IR) divergences are done by dimensional regularization. Renormalization of the strong coupling constant, α_s, is done in the $\overline{\text{MS}}$ scheme, heavy quark contribution can be removed via zero-momentum subtraction and unstable particles are treated in the complex-mass scheme. OpenLoops comes with an extensive amplitude library containing all matrix elements needed for NLO QCD corrections. Moreover, it includes colour and helicity correlators and real radiation as well as loop-squared amplitudes for hundreds of LHC processes. For lepton collisions the LHC libraries may usually be used, but for processes with massive quarks in the final state there are special dedicated libraries.

3 Top quark physics

Because of its large mass, the top quark plays a special role in the Standard Model (SM) and extensions thereof. With a mass around 173 GeV it is heavier than the W boson and may therefore decay semi-weakly as $t \to Wb$. Therefore, it has a very short lifetime and decays before hadronization. A special interest in the top quark comes from Higgs physics where it is the only quark whose Yukawa coupling to the Higgs boson is order of unity. The unique phenomenology of the top quark provides a great testing ground for perturbative and non-perturbative QCD. Detailed calculations and measurements of top quark parameters such as mass, couplings, decay branching ratios etc. may provide important information about interactions at the electroweak breaking scale and about physics beyond SM.

3.1 Top quark decay

Since the top quark decays semi-weakly we may treat the W boson as an on-shell final state particle when calculating $\Gamma(t \to bW)$. The matrix element is given by

$$\mathcal{M} = \frac{g_w}{\sqrt{2}} \epsilon^*_\mu(p_W) \bar{u}(p_b) \gamma^\mu \frac{1}{2}(1 - \gamma^5) u(p_t) \tag{3.1}$$

where $g_W = e/\sin\theta_W$ and ϵ^*_μ is the polarization vector of the W boson. Going to the CoM frame of the top quark, defining the b-quark direction as the z-axis and assuming $m_b = 0$ the different four-momenta are

$$\begin{aligned} p_t &= (m_t, 0, 0, 0) \\ p_b &= (p^*, 0, 0, p^*) \\ p_W &= (E^*, 0, 0 - p^*) \end{aligned} \tag{3.2}$$

where, since W is on-shell, $E^{*2} = p^{*2} + m_W^2$. Since m_b is taken to zero the helicity and chiral states of the b-quark is equivalent and consequently, since the weak interaction only couples to left-handed chiral states, only left-handed chiral/helicity states may be produced. The chiral spinor for the b-quark is

$$u_L(p_b) = \sqrt{p^*}(0, 1, 0, -1). \tag{3.3}$$

and the two different spin states of the t-quark have the spinors

$$u_1(p_t) = \sqrt{(2m_t)}(1, 0, 0, 0) \tag{3.4}$$

$$u_2(p_t) = \sqrt{(2m_t)}(0, 1, 0, 0). \tag{3.5}$$

Finally the W boson has three polarization states;

$$\begin{aligned} \epsilon^*_+(p_W) &= -\frac{1}{\sqrt{2}}(0, 1, -i, 0) \\ \epsilon^*_-(p_W) &= \frac{1}{\sqrt{2}}(0, 1, i, 0) \\ \epsilon^*_L(p_W) &= \frac{1}{m_W}(-p^*, 0, 0, E^*). \end{aligned} \tag{3.6}$$

The only combinations of spinors and polarizations that are non-zero are those that conserve angular momentum; giving only two non-zero contributions to the matrix element

$$\mathcal{M}_1 = \frac{g_W}{\sqrt{2}}\epsilon^*_{+,\mu}(p_W)(\bar{u}_L(p_b)\gamma^\mu u_1(p_t)) = -g_W\sqrt{2m_t p^*} \tag{3.7}$$

$$\mathcal{M}_2 = \frac{g_W}{\sqrt{2}}\epsilon^*_{L,\mu}(p_W)(\bar{u}_L(p_b))\gamma^\mu u_2(p_t) = -\frac{g_W m_t}{m_W}\sqrt{m_t p^*}. \tag{3.8}$$

The spin-averaged matrix element squared is therefore

$$\left\langle|\mathcal{M}|^2\right\rangle = \frac{1}{2}\left(|\mathcal{M}_1|^2 + |\mathcal{M}_2|^2\right) = \frac{1}{2}g_W^2 m_t p^* \left(2 + \frac{m_t^2}{m_W^2}\right). \tag{3.9}$$

To get the total decay width we just have to integrate over phase space

$$\Gamma = \frac{p^*}{32\pi^2 m_t^2}\int \left\langle|\mathcal{M}|^2\right\rangle d\Omega = \frac{g_W^2 p^{*2}}{16\pi m_t}\left(2 + \frac{m_t^2}{m_W^2}\right) \tag{3.10}$$

which may also be written as

$$\Gamma^{\mathrm{LO}}(t \to bW) = \frac{G_F m_t^3}{8\pi\sqrt{2}}\left(1 - \frac{m_W^2}{m_t^2}\right)^2\left(1 + \frac{2m_W^2}{m_t^2}\right). \tag{3.11}$$

To the next-to-leading order the width is given by [14](neglecting terms of order m_b^2/m_t^2, α_s^2 and $\alpha_s m_W^2/\pi m_t^2$)

$$\Gamma^{\mathrm{NLO}}(t \to bW) = \Gamma^{\mathrm{LO}}\left[1 - \frac{2\alpha_s}{3\pi}\left(\frac{2\pi^2}{3} - \frac{5}{2}\right)\right]. \tag{3.12}$$

Using $m_t = 173,3$ GeV and $\alpha_s(m_Z) = 0.118$ the lifetime of the top quark is approximately $5 \cdot 10^{-25}$s which is about one tenth of the characteristic QCD time scale and thus no $t\bar{t}$ quarkonium should be created in collisions.

3.2 Cross section for $t\bar{t}$ production

The Born amplitude for $e^+e^- \to t\bar{t}$ is an s-channel process with γ/Z exchange, see Fig. 1. For the full cross section both contributions have to be included, but the purpose of this section is to calculate NLO QCD contributions and show the appearance and cancellation of divergences, thus we will only study the γ-exchange for simplicity. A complete $\mathcal{O}(\alpha_S)$ calculation, where the Z-exchange is included can be found in [15–17]. Let p and q be the four-momentum of the electron and positron respectively and let p' and q' be the four-momentum of the top and anti-top quark. Neglecting the electron mass the matrix element for the Born process is

$$\mathcal{M}_{\mathrm{LO}} = \frac{e^2 Q_e Q_t}{s}\bar{v}(q)\gamma^\mu u(p)\bar{u}(p')\gamma_\mu v(q')\delta_{ij} \tag{3.13}$$

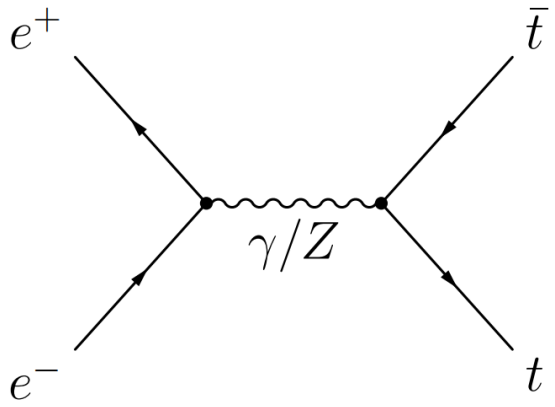

Figure 1: The s-channel Born process for $e^+e^- \to t\bar{t}$.

where i and j are the colour indices of the outgoing quarks. In the CoM frame of the colliding leptons the four-momenta are

$$\begin{aligned} p &= \frac{\sqrt{s}}{2}(1,0,0,1) \\ q &= \frac{\sqrt{s}}{2}(1,0,0,-1) \\ p' &= \frac{\sqrt{s}}{2}(1,\beta\sin\theta,0,\beta\cos\theta) \\ q' &= \frac{\sqrt{s}}{2}(1,-\beta\sin\theta,0,-\beta\cos\theta) \end{aligned}$$

where $s = (p+q)^2$ and

$$\beta = \sqrt{1 - \frac{4m_t^2}{s}}.$$

In $d = 4 - 2\epsilon$ dimensions the square amplitude is

$$|\mathcal{M}_{\rm LO}|^2 = 64\pi^2\alpha^2 Q_t^2 N_c \left[2(1-\epsilon) + \beta^2(\cos^2\theta - 1)\right] \tag{3.14}$$

where the colour factor is $N_c = 3$. To get the corresponding cross section we need the two-body phase space

$$d\Phi_2 = \frac{2^{2\epsilon}}{16\pi}\left(\frac{4\pi}{s}\right)^{\epsilon}\beta^{1-2\epsilon}\frac{1}{\Gamma(1-\epsilon)}\int_0^{\pi}\sin^{1-2\epsilon}\theta d\theta \tag{3.15}$$

which yields the cross section

$$\begin{aligned} \sigma_{\rm LO} &= \frac{1}{8s}\int |\mathcal{M}_{\rm LO}|^2 d\Phi_2 \\ &= \frac{\beta}{128\pi s}\int_{-1}^{1} d\cos\theta |\mathcal{M}_{LO}|^2 + \mathcal{O}(\epsilon) \\ &= \frac{2\pi N_c\alpha^2 Q_t^2}{3s}\beta(3-\beta^2) + \mathcal{O}(\epsilon). \end{aligned} \tag{3.16}$$

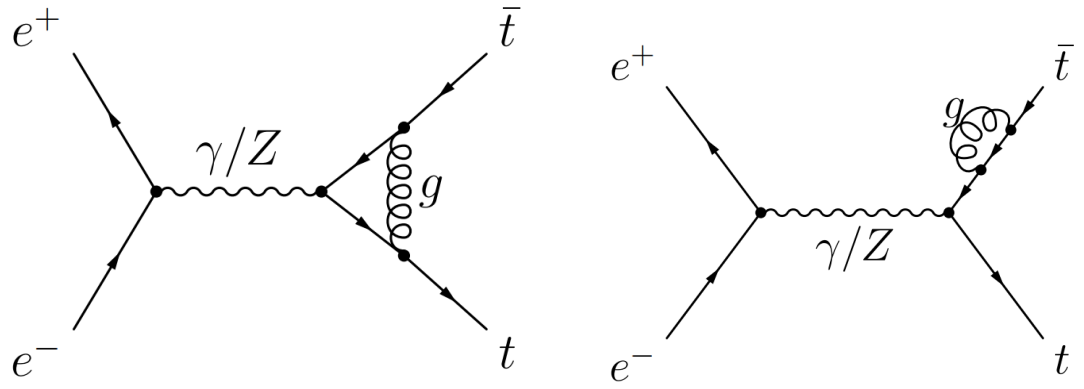

(a) (b)

Figure 2: The two virtual contributions to $\sigma_{\text{NLO}}(e^+e^- \to t\bar{t})$. (a) is the vertex correction and (b) the wave function renormalization.

To calculate the cross section at NLO we need both real and virtual contributions to the LO cross section,

$$\sigma_{\text{NLO}} = \sigma_{\text{LO}} + \sigma_{\text{virtual}} + \sigma_{\text{real}}. \tag{3.17}$$

The one-loop virtual contributions consists of a vertex correction and a wave function renormalization, see Fig. 2. For the virtual corrections we are not interested in the incoming leptons so we may write the amplitude for the vertex correction as

$$\mathcal{M}_{\text{vertex}} = eQ_e\bar{v}(q)\gamma_\nu u(p)\frac{1}{s}\Gamma^\nu(p',q') \tag{3.18}$$

with

$$\Gamma_\nu(p',q') = (-eQ_t)\delta_{ij}g_s^2 C_F[N]\bar{u}(p')\left[A\frac{(p'+q')_\nu}{2m_t} + B\gamma_\nu\right]v(q') \tag{3.19}$$

where we have chosen the normalization

$$[N] = \frac{1}{16\pi^2}\left(\frac{4\pi\mu^2}{m_t^2}\right)^\epsilon \Gamma(1+\epsilon) \tag{3.20}$$

and have the colour factor

$$C_F = \frac{N_c^2 - 1}{2N_c} = \frac{4}{3}. \tag{3.21}$$

The parameter μ is the renormalization scale. Explicit calculations of A and B can be done, see [15–17], but for us it is enough to notice that A is independent of ϵ and that we may write B as

$$B = \frac{B_\epsilon}{\epsilon} + B_{\text{finite}}. \tag{3.22}$$

To get the $\mathcal{O}(\alpha_s)$ contribution to the virtual cross section we calculate the interference term of the vertex amplitude and the leading order amplitude, this yields

$$\begin{aligned}\sigma_{\text{vertex}} &= 2\frac{1}{8s}\int d\Phi_2 \mathcal{M}_{\text{LO}}\mathcal{M}^*_{\text{vertex}} \\ &= \frac{\alpha_s}{2\pi}\left(\frac{4\pi\mu^2}{m_t^2}\right)^\epsilon C_F\Gamma(1+\epsilon)\sigma_{\text{LO}}\left[\frac{B_\epsilon}{\epsilon} + B_{\text{finite}}\right].\end{aligned} \tag{3.23}$$

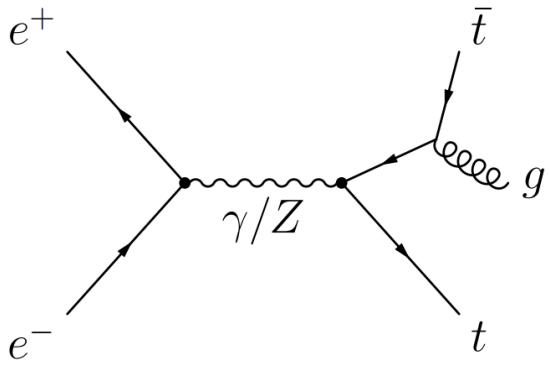

Figure 3: A Feynman diagram for real gluon emission.

Note that the $\mathcal{O}(\epsilon)$ term from σ_{LO} together with B_ϵ/ϵ forms a finite term. The wave function renormalization, Fig. 2(b) can easily be dealt with using on-shell renormalization, giving the cross section

$$\sigma_Z = 2\delta Z_{tt}\sigma_{\text{LO}} \tag{3.24}$$

where

$$\begin{aligned}\delta Z_{tt} &= \left.\frac{\partial \Pi(p^2)}{\partial p^2}\right|_{p^2=m_t^2} \\ &= -\frac{\alpha_S}{4\pi}\left(\frac{4\pi\mu^2}{m_t^2}\right)^\epsilon C_F \Gamma(1+\epsilon)\left[\frac{3}{\epsilon}+4\right].\end{aligned} \tag{3.25}$$

With the total virtual contribution now given by

$$\begin{aligned}\sigma_{\text{virtual}} &= \sigma_{\text{vertex}} + \sigma_Z \\ &= \sigma_{\text{LO}}\frac{\alpha_s}{2\pi}\Gamma(1+\epsilon)C_F\left(\frac{4\pi\mu^2}{m_t^2}\right)^\epsilon\left[(-3+B_\epsilon)\frac{1}{\epsilon}-4+B_{\text{finite}}\right].\end{aligned} \tag{3.26}$$

What is left now, to get the total cross section at NLO, is the real contribution which comes from real gluon emission, see Fig. 3. Calculating this contribution is even more elaborative than the virtual contribution (e.g. we now have a three-body phase space), so here we will only focus on the divergences. Note that because of the massive top quark, the diagram in Fig. 3 has no collinear singularity. However, it has a soft (IR) singularity as the energy of the emitted gluon approaches zero. This singularity can be regulated with phase space slicing (PSS) [17]. The idea is that we split the phase space in one soft and one hard part such that

$$\sigma_{\text{real}} = \sigma_{\text{soft}} + \sigma_{\text{hard}} \tag{3.27}$$

where σ_{hard} is finite and the soft singularity is contained in σ_{soft}, this introduces an arbitrary parameter δ_s describing where the phase space is cut, clearly σ_{real} must be independent of this parameter. Calculating the three-body phase space integral for the soft contribution will after some pages of work give

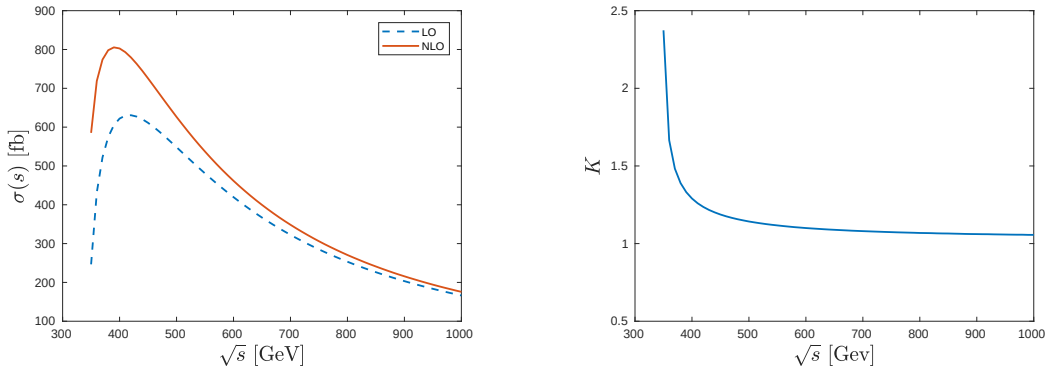

(a) (b)

Figure 4: (a) the cross section for $e^+e^- \to t\bar{t}$ calculated at LO and NLO using WHIZARD. (b) the K-factor defined as $K = \sigma_{\text{NLO}}/\sigma_{\text{LO}}$.

$$\sigma_{\text{soft}} = \sigma_{\text{LO}} \frac{\alpha_s}{2\pi} C_F \left(\frac{4\pi\mu^2}{s}\right)^{\epsilon} \frac{\Gamma(1-\epsilon)}{\Gamma(1-2\epsilon)} \left[\frac{C_\epsilon}{\epsilon} + C_{\text{finite}}\right]. \tag{3.28}$$

We now have the total NLO cross section

$$\sigma_{\text{NLO}} = \sigma_{\text{LO}} + \sigma_{\text{virtual}} + \sigma_{\text{soft}} + \sigma_{\text{hard}} \tag{3.29}$$

where the hard and leading order contributions are finite while both the virtual and soft contribution as a $1/\epsilon$ singularity. Using the explicit expressions for B_ϵ and C_ϵ these singularities actually cancels [17] and we are left with a finite expression. The cross section for $e^+e^- \to t\bar{t}$ is shown in Fig. 4, both at LO and NLO, calculated using WHIZARD.

4 Validation of NLO QCD for lepton collisions

4.1 Setup

As input parameters we used the following masses (all others are set to zero)

$$m_Z = 91.188 \text{ GeV}, \quad m_W = 80.419002 \text{ GeV}, \quad m_H = 125.0 \text{ GeV}$$
$$m_t = 173.2 \text{ GeV}, \quad m_\tau = 1.777 \text{ GeV}.$$

The widths of the gauge bosons, the top quark and Higgs are set to zero. We use $G_F = 1.16639 \cdot 10^{-5}$ GeV^{-2} together with $\alpha_s(m_Z) = 0.118$ where the running includes five colours. For the electron collisions we have $\sqrt{s} = 1$ TeV.

4.2 Validation

In Table 1 a sample of cross section calculations at LO and NLO is shown together with the MadGraph5 results from [9].

Table 1: Cross section calculations at LO and NLO using WHIZARD and compared to MadGraph5 results from [9].

	MG5			WHIZARD		
Final state	σ^{LO}[fb]	σ^{NLO}[fb]	K	σ^{LO}[fb]	σ^{NLO}[fb]	K
jj	622.3(5)	639(1)	1.02684	622.83(7)	642.3(1)	1.03126
$b\bar{b}$	91.89(4)	92.8(3)	1.0099	92.311(8)	94.72(9)	1.0259
$t\bar{t}$	166.2(2)	174.5(6)	1.0499	166.41(1)	174.86(4)	1.0508
$t\bar{t}t\bar{t}$	$6.46(2)\cdot10^{-4}$	$12.21(5)\cdot10^{-4}$	1.89	$6.485(15)\cdot10^{-4}$	$12.16(3)\cdot10^{-4}$	1.8769
$b\bar{b}b\bar{b}$	$1.644(3)\cdot10^{-1}$	$3.60(2)\cdot10^{-1}$	2.1951	$1.63(2)\cdot10^{-1}$	$3.5(8)\cdot10^{-1}$	1.875
$t\bar{t}b\bar{b}$	$1.819(3)\cdot10^{-1}$	$2.92(1)\cdot10^{-1}$	1.61326	$1.84(1)\cdot10^{-1}$	$5.46(3)\cdot10^{-1}$	3
$t\bar{t}j$	48.13(5)	52.76(22)	1.0811	48.32(16)	55.93(53)	1.4583
$t\bar{t}H$	2.018(3)	1.911(6)	0.945545	2.030(3)	1.921(3)	0.94581
$t\bar{t}\gamma$	12.70(2)	13.35(4)	1.05512	–	–	–
$t\bar{t}Z$	4.612(6)	4.949(14)	1.06291	–	–	–
$t\bar{t}HZ$	$3.600(6)\cdot10^{-2}$	$3.579(13)\cdot10^{-2}$	1	–	–	–
$t\bar{t}\gamma Z$	$2.212(3)\cdot10^{-1}$	$2.364(6)\cdot10^{-1}$	1.06787	–	–	–
$t\bar{t}\gamma H$	$9.756(16)\cdot10^{-2}$	$9.423(32)\cdot10^{-2}$	0.9691	–	–	–
$t\bar{t}\gamma\gamma$	0.3650(8)	0.3833(13)	1.04110	–	–	–
$t\bar{t}ZZ$	$3.788(4)\cdot10^{-2}$	$4.007(13)\cdot10^{-2}$	0.9475	–	–	–
$t\bar{t}HH$	$1.358(1)\cdot10^{-2}$	$1.206(3)\cdot10^{-2}$	0.88971	–	–	–
$t\bar{t}W^+W^-$	0.1372(3)	0.1540(6)	1.12409	–	–	–
$t\bar{t}W^\pm jj$	$2.400(4)\cdot10^{-4}$	$3.723(12)\cdot10^{-4}$	1.5417	–	–	–
jjj	340.1(2)	317(2)	0.93235	–	–	–
$jjjj$	104.7(1)	109.0(6)	1.03810	–	–	–
$t\bar{t}t\bar{t}j$	$2.719(5)\cdot10^{-5}$	$5.338(27)\cdot10^{-5}$	1.94853	$2.702(15)\cdot10^{-5}$	$4.055(29)\cdot10^{-5}$	1.4815
$t\bar{t}Hj$	0.2533(3)	0.2658(9)	1.051383	0.2555(12)	0.2686(15)	1.0385
$t\bar{t}\gamma j$	2.355(2)	2.617(10)	1.11017	–	–	–
$t\bar{t}Zj$	0.6159(6)	0.6940(28)	1.12013	–	–	–

5 Concluding remarks

The validations shown in Table 1 have not been preformed for all processes. The goal would be to do all the tests done with previous versions of WHIZARD, see Appendix A. For the calculated processes the agreement between MadGraph5 and WHIZARD is for the most part satisfactory, except for NLO $t\bar{t}b\bar{b}$ and NLO $t\bar{t}t\bar{t}j$.

Acknowledgments

I would like to thank Jürgen Reuter, Christian Weiss and Vincent Rothe for their support throughout this work.

References

[1] H. Baer, T. Barklow, K. Fujii, Y. Gao, A. Hoang, S. Kanemura et al., *The International Linear Collider Technical Design Report - Volume 2: Physics*, 1306.6352.

[2] L. Linssen, A. Miyamoto, M. Stanitzki and H. Weerts, *Physics and Detectors at CLIC: CLIC Conceptual Design Report*, 1202.5940.

[3] G. Degrassi, S. Di Vita, J. Elias-Miró, J. R. Espinosa, G. F. Giudice, G. Isidori et al., *Higgs mass and vacuum stability in the standard model at nnlo*, *JHEP* **2012** (Aug, 2012) 098.

[4] A. V. Bednyakov, B. A. Kniehl, A. F. Pikelner and O. L. Veretin, *Stability of the electroweak vacuum: Gauge independence and advanced precision*, *Phys. Rev. Lett.* **115** (Nov, 2015) 201802.

[5] M. Vos et al., *Top physics at high-energy lepton colliders*, 1604.08122.

[6] M. Moretti, T. Ohl and J. Reuter, *O'Mega: An Optimizing matrix element generator*, hep-ph/0102195.

[7] W. Kilian, T. Ohl and J. Reuter, *WHIZARD—simulating multi-particle processes at LHC and ILC*, *Eur. Phys. J. C* **71** (Sep, 2011) 1742.

[8] F. Cascioli, P. Maierhofer and S. Pozzorini, *Scattering Amplitudes with Open Loops*, *Phys. Rev. Lett.* **108** (2012) 111601, [1111.5206].

[9] J. Alwall, R. Frederix, S. Frixione, V. Hirschi, F. Maltoni, O. Mattelaer et al., *The automated computation of tree-level and next-to-leading order differential cross sections, and their matching to parton shower simulations*, *JHEP* **07** (Jul, 2014) 079.

[10] T. Ohl, *Vegas revisited: Adaptive Monte Carlo integration beyond factorization*, *Comput. Phys. Commun.* **120** (1999) 13–19, [hep-ph/9806432].

[11] T. Ohl, *CIRCE version 1.0: Beam spectra for simulating linear collider physics*, *Comput. Phys. Commun.* **101** (1997) 269–288, [hep-ph/9607454].

[12] S. Frixione, Z. Kunszt and A. Signer, *Three jet cross-sections to next-to-leading order*, *Nucl. Phys.* **B467** (1996) 399–442, [hep-ph/9512328].

[13] R. Frederix, S. Frixione, F. Maltoni and T. Stelzer, *Automation of next-to-leading order computations in QCD: The FKS subtraction*, *JHEP* **10** (2009) 003, [0908.4272].

[14] M. Jeżabek and J. K *QCD corrections to semileptonic decays of heavy quarks*, *Nucl. Phys. B* **314** (1989) 1 – 6.

[15] J. Jersák, E. Laermann and P. M. Zerwas, *Electroweak production of heavy quarks in e^+e^- annihilation*, *Phys. Rev. D* **25** (Mar, 1982) 1218–1228.

[16] V. Ravindran and W. L. van Neerven, *Second order QCD corrections to the forward - backward asymmetry in e+ e- collisions*, *Phys. Lett.* **B445** (1998) 214–222, [hep-ph/9809411].

[17] B. W. Harris and J. F. Owens, *The Two cutoff phase space slicing method*, *Phys. Rev.* **D65** (2002) 094032, [hep-ph/0102128].

A Earlier WHIZARD validation

Here we show an earlier set of WHIZARD validations.

Validation of NLO QCD for Lepton Collisions

24 / 33

Final state	σ^{LO}[fb]	MG5_aMC σ^{NLO}[fb]	K	σ^{LO}[fb]	WHIZARD σ^{NLO}[fb]	K
jj	622.3(5)	639(1)	1.02684	622.73(4)	639.7(2)	1.0272
$b\bar{b}$	92.37(6)	94.89(1)	1.02728	92.32(1)	94.78(7)	1.0266
$t\bar{t}$	166.2(2)	174.5(6)	1.04994	166.4(1)	175.1(1)	1.0522
$t\bar{t}t\bar{t}$	$6.45(1)\cdot 10^{-4}$	$12.21(5)\cdot 10^{-4}$	1.89302	$6.463(2)\cdot 10^{-4}$	$12.16(2)\cdot 10^{-4}$	1.8814
$b\bar{b}b\bar{b}$	$1.644(3)\cdot 10^{-1}$	$3.60(1)\cdot 10^{-1}$	2.1897	$1.64(2)\cdot 10^{-1}$	$3.67(4)\cdot 10^{-1}$	2.2378
$t\bar{t}b\bar{b}$	$1.819(3)\cdot 10^{-1}$	$2.92(1)\cdot 10^{-1}$	1.6052	$1.86(1)\cdot 10^{-1}$	$2.93(2)\cdot 10^{-1}$	1.5752
$t\bar{t}j$	48.13(5)	53.43(1)	1.11012	48.3(2)	53.66(9)	1.1109
$t\bar{t}H$	2.018(3)	1.911(6)	0.947	2.022(3)	1.913(3)	0.9461
$t\bar{t}\gamma$	12.7(2)	13.3(4)	1.04726	12.71(4)	13.78(4)	1.0841
$t\bar{t}Z$	4.642(6)	4.95(1)	1.06636	4.64(1)	4.94(1)	1.0646
$t\bar{t}HZ$	$3.600(6)\cdot 10^{-2}$	$3.58(1)\cdot 10^{-2}$	0.99445	$3.596(1)\cdot 10^{-2}$	$3.581(2)\cdot 10^{-2}$	0.9958
$t\bar{t}\gamma Z$	0.2212(3)	0.2364(6)	1.06873	0.220(1)	0.240(2)	1.0909
$t\bar{t}\gamma H$	$9.75(1)\cdot 10^{-2}$	$9.42(3)\cdot 10^{-2}$	0.96614	$9.748(6)\cdot 10^{-2}$	$9.58(7)\cdot 10^{-2}$	0.9827
$t\bar{t}\gamma\gamma$	0.383(5)	0.416(2)	1.08618	0.382(3)	0.420(3)	1.0995
$t\bar{t}ZZ$	$3.788(4)\cdot 10^{-2}$	$4.00(1)\cdot 10^{-2}$	1.05597	$3.756(4)\cdot 10^{-2}$	$4.005(2)\cdot 10^{-2}$	1.0663
$t\bar{t}HH$	$1.358(1)\cdot 10^{-2}$	$1.206(3)\cdot 10^{-2}$	0.888	$1.367(1)\cdot 10^{-2}$	$1.218(1)\cdot 10^{-2}$	0.8909
tW^+W^-	0.1372(3)	0.1540(6)	1.1225	0.1370(4)	0.1538(4)	1.1225
$tW^{\pm}jj$	$2.400(4)\cdot 10^{-4}$	$3.72(1)\cdot 10^{-4}$	1.54999	$2.41(1)\cdot 10^{-4}$	$3.74(2)\cdot 10^{-4}$	1.5518
jjj	340.1(2)	316(2)	0.92914	342.4(5)	319(1)	0.9316
$jjjj$	104.7(1)	109.0(6)	1.04106	105.1(4)	118(1)	1.1227
$ttt\bar{t}j$	$2.719(5)\cdot 10^{-5}$	$5.34(3)\cdot 10^{-5}$	1.96394	$2.722(1)\cdot 10^{-5}$	$4.471(5)\cdot 10^{-5}$	1.6425
$t\bar{t}Hj$	0.2533(3)	0.2658(9)	1.04935	0.254(1)	0.307(1)	1.2087
$t\bar{t}\gamma j$	2.355(2)	2.62(1)	1.11253	2.47(1)	3.14(2)	1.2712
$t\bar{t}Zj$	0.6059(6)	0.694(3)	1.14548	0.610(4)	0.666(5)	1.0918

J.R.Reuter The event generator WHIZARD Physics for CLIC, CERN, 18.07.17